Accepted Article

Title: Framework Effects on Activation and Functionalisation of
Methane in Zinc-Exchanged Zeolites

Authors: Meera A Shah, Sam Raynes, David C Apperley, and Russell
A. Taylor

This manuscript has been accepted after peer review and appears as an
Accepted Article online prior to editing, proofing, and formal publication
of the final Version of Record (VoR). This work is currently citable by
using the Digital Object Identifier (DOI) given below. The VoR will be
published online in Early View as soon as possible and may be different
to this Accepted Article as a result of editing. Readers should obtain
the VoR from the journal website shown below when it is published
to ensure accuracy of information. The authors are responsible for the
content of this Accepted Article.

RESEARCH ARTICLE

Framework Effects on Activation and Functionalisation of Methane in Zinc-Exchanged Zeolites

Meera A. Shah,[a] Samuel Raynes,[a] Dr David C. Apperley,[a] and Dr Russell A. Taylor*[a]

Abstract: The first selective oxidation of methane to methanol is reported herein for zinc-exchanged MOR (Zn/MOR). Under identical conditions, Zn/FER and Zn/ZSM-5 both form zinc formate and methanol. Selective methane activation to form [Zn-CH₃]⁺ species was confirmed by ^{13}C MAS NMR spectroscopy for all three frameworks. The percentage of active zinc sites, measured through quantitative NMR spectroscopy studies, varied with the zeolite framework and was found to be ZSM-5 (5.7%), MOR (1.2%) and FER (0.8%). For Zn/MOR, two signals were observed in the ^{13}C MAS NMR spectrum, resulting from two distinct [Zn-CH₃]⁺ species present in the 12 MR and 8 MR side pockets, as supported by additional NMR experiments. The observed products of oxidation of the [Zn-CH₃]⁺ species are shown to depend on the zeolite framework type and the oxidative conditions used. These results lay the foundation for developing structure-function correlations for methane conversion over zinc-exchanged zeolites.

Introduction

To date, the selective partial oxidation of methane to methanol remains a 'holy grail' of catalysis.[1] This highly sought after catalytic reaction could provide a more efficient approach to the industrially practiced method of methane to methanol via syngas (CO and H₂).[2] It has been reported that 60% of the capital cost of a methane to methanol facility stems from the syngas plant.[2a] Additionally, given that nature has mastered this conversion through methantropic bacteria, it is tantalising to hope that a similar process could be engineered through modern chemical methods.[3]
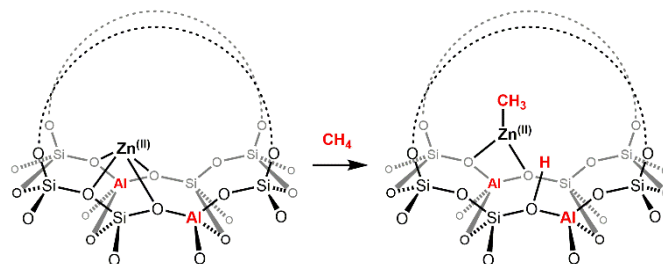
Metal-exchanged zeolites have shown great potential for the direct conversion of methane to methanol.[4] In particular, copper-modified zeolites have been intensely studied especially due to catalyst activation being possible under an O₂ atmosphere.[3c, 4b, 5] The radical based mechanism operative in Cu-modified zeolites has been well established[6] and confinement effects within zeolites containing small pores, promoting the partial oxidation of methane, have traditionally resulted in the greatest methanol yields.[4c, 7] In particular, the framework MOR, with 8MR side pockets, has particularly shown high selectivity and yield for methanol production from methane.[8]

In 2004, Kazansky *et al.* reported the heterolytic bond dissociation of CH₄ over zinc-modified ZSM-5.[9] A major advantage of these zinc based systems is the ability to form active species without an initial high temperature oxidation step as

required for iron and copper modified zeolites.[3c] As evidenced by DRIFTS and MAS NMR studies, methane activation at Zn²⁺ exchanged ZSM-5 zeolites is generally accepted to result in heterolytic cleavage of the C-H bond in methane, leading to the formation of a [Zn-CH₃]⁺ species and a new BAS (Scheme 1)[9-10] Spectroscopic and theoretical studies have shown that the mechanism proceeds through initial complexation of methane to the Lewis acidic Zn²⁺ species, with the CH₄ δ(C-H) orbital donating electron density into the Zn-4s orbital (methane sigma complex), after which the framework oxygen atom acts as a Lewis base, leading to C-H bond cleavage.[9-10, 11]

Reactivity of the resulting zinc methyl fragment with other small molecules has been explored, in the context of stoichiometric reactions as well as potential catalytic applications. Addition of dioxygen to [Zn-CH₃]⁺/ZSM-5 at ambient and elevated temperature has been shown to result in the formation of zinc methoxy and zinc formate species, as monitored through NMR spectroscopic studies. [10b, 12] On this basis, it has been shown that the chemical reactivity of [Zn-CH₃]⁺ within ZSM-5, with molecules such as CO, CO₂ and H₂O, has been found to be very similar to that of organozinc compounds.[10b, 12-13]

Whilst methane activation and oxidation has been explored over zinc-modified ZSM-5, the effect of the zeolite framework on the activation and subsequent functionalisation steps has not yet been investigated. To this end we have conducted a series of studies exploring the C-H activation of methane in three different zinc modified frameworks, MFI, MOR and FER, which have intrinsically different micropore topologies. We report that selective methane activation occurs over ZSM-5, FER and MOR zeolites that have been modified by zinc vapour at elevated temperature. Solid state NMR studies have shown that two distinct [Zn-CH₃]⁺ species are formed in MOR, due to the very different topological environments within the MOR Framework. Additionally we show that the zeolite framework can influence the observed product(s) when [Zn-CH₃]⁺ reacts with O₂ or air. Uniquely, a zinc methoxy species is the sole observable carbon containing product when the [Zn-CH₃]⁺ species is exposed to air for Zn/MOR. These results point at the ability of the framework topology to effect the outcome of the reaction in methane oxidation as mediated by zinc exchanged zeolites, hitherto unreported.

[a] Meera A. Shah, Samuel Raynes, Dr David C. Apperley and Dr Russell A. Taylor
Department of Chemistry, Durham University, South Road, Durham, DH1 3LE
E-mail: russell.taylor@durham.ac.uk

Supporting information for this article is given via a link at the end of the document.

Scheme 1: C–H activation step for dissociative adsorption of methane over Zn²⁺ forming a [Zn-CH₃]⁺ and new BAS

RESEARCH ARTICLE

Results and Discussion

The effect of zeolite framework on CH₄ activation

Zinc exchanged zeolites of three differing frameworks, H-ZSM-5, NH₄-FER and H-MOR, were prepared by chemical vapour deposition (CVD) with an excess of zinc metal (100:1 Zn:Al) in a custom designed u-shaped quartz tube (Figure SI1). CVD was carried out at 500 °C under reduced pressure (less than 10^{-2} mbar). This was followed by methane activation at 250 °C, based on conditions reported previously by Stepanov *et al.*.[10b] Particular care was taken to prevent aerial oxidation, especially after CH₄ exposure, hence, all the samples was transferred to a glovebox and packed into an NMR rotor in an inert environment (Ar). An additional sample prepared by aqueous ion exchange (IE) was also prepared to provide a comparison to the CVD samples.

CVD methods introduce predominantly Zn^{2+} cations to high exchange levels.[9-10, 10c] Under certain CVD conditions, additional zinc species have been detected (Zn^+,[14] $[Zn_2]^{2+}$ [15]) but these have not been reported to react with methane. To investigate the level of exchange of the BAS for zinc cations after CVD treatment with zinc metal vapour, ¹H NMR and ¹H-²⁷Al REAPDOR NMR spectroscopic experiments were conducted on the parent zeolites and the products of the CVD reaction. The ¹H-²⁷Al REAPDOR experiment probes the aluminium-proton separation by reintroducing the dipolar coupling that is removed by magic angle spinning, thus enabling the determination of which signals in the ¹H spectrum are closely associated with ²⁷Al.[16] For the parent zeolites, the signal at 4.0 ppm corresponding to BAS or 6.6 ppm corresponding to $[NH_4]^+$ (in the case of FER), is clearly associated with Al as determined by the appearance in the ¹H-²⁷Al REAPDOR difference spectrum (MOR: Figure 1b; ZSM-5: Figure SI3a; FER: Figure SI4a). Upon exposure to zinc vapour, this peak either disappears indicative of full exchange with Zn^{2+} (MOR,
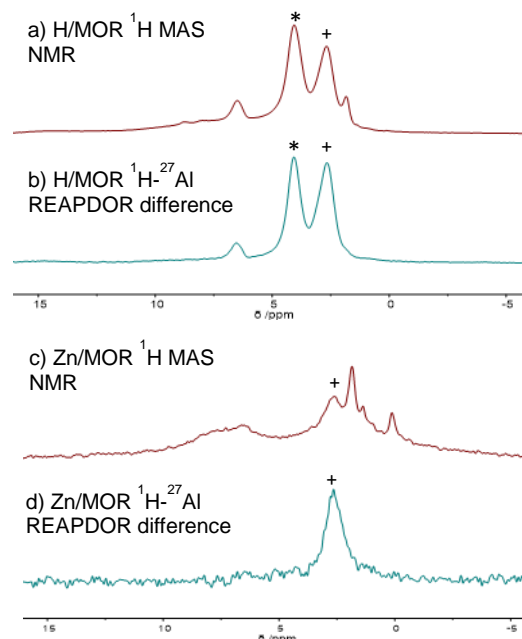

Figure 1: ¹H MAS NMR (a and c) and ¹H-²⁷Al REAPDOR difference spectra (b and d) for MOR framework. Left: parent zeolite. Right: Zn MOR (after CVD). *Signal at 4 ppm related to BAS disappears upon vapour deposition of zinc metal. ⁺Signal at 2.5 ppm associated with extraframework Al. Peak at 0 ppm due to adventitious silicon vacuum grease.

Figure 1c and d, and FER, Figure SI4b) or decreases drastically (ZSM-5) (Figure SI2b).

Elemental analysis (Table 1) was also used to determine the extent of zinc exchange after CVD and ion exchange. The Zn/Al ratios were found to be over the theoretical maximum exchange value of 0.5 for all CVD samples but values greater than 0.5 have previously been observed and attributed to excess Zn(0) present within the sample.[17] Brunauer−Emmett−Teller (BET) measurements were carried out in order to confirm that the zinc

Table 1: Elemental analysis, BET measurements and C-H activation results for zinc exchanged zeolites

Sample (given Si/Al)	Measured Si/Al*	Zn/Al#	BET / m²/g	Successful C-H activation	Percentage Zn active sites ‡
H-ZSM-5 (15)	12.5	-	435.0 ± 0.2	N	-
NH₄-ZSM-5 (12.5)	11.6	-	447.3 ± 0.4	N	-
H-MOR (10)	7.9	-	542.2 ± 1.6	N	-
NH₄-FER (10)	11.2	-	404.1 ± 0.5	N	-
Zn/ZSM-5 (15)	12.5	0.78	303.7 ± 0.4	-	-
Zn/CH₄/ZSM-5 (15)	12.5	0.73		Y	5.7 %
Zn/FER (10)	11.2	0.69	305.5 ± 0.3	-	-
Zn/CH₄/FER (10)	11.2	0.77		Y	0.8 %
Zn/MOR (10)	7.9	0.74	421.9 ± 0.6	-	-
Zn/CH₄/MOR (10)	7.9	0.75		Y	1.2 %
Zn/H-ZSM-5-IE (12.5)	11.6	0.45	377.3 ± 0.3	Y	0.5 %

*determined by WDXRF, # determined by ICP-OES, ‡ NMR quantification with hexamethylbenzene (HMB) as a standard. Percentage of zinc sites that result in $[Zn-CH_3]^+$ species. Values given are an average of two independent experiments. Details on quantification can be found in the SI.

introduction methods did not cause pore blockage of the zeolites, particularly for MOR, which has a unidirectional pore system. A reduction in surface area is observed due to the presence of extraframework zinc (Table 1), similar to the results of Pidko *et al.*.[17] The materials have been additionally analysed by powder X-ray diffraction analysis (pXRD) and ^{29}Si NMR spectroscopy to determine the effect of CVD on the zeolite structure. Figure 2 compares the pXRD patterns of the parent zeolites with the pXRD patterns after vapour deposition confirming that after CVD of zinc metal the framework remains intact. Furthermore, no additional diffraction peaks corresponding to zinc metal were observed in the pXRD patterns. No additional extra framework Al was observed after zinc CVD as determined through ^{27}Al MAS NMR spectroscopy (Figures SI8-11). Analysis by ^{1}H-^{29}Si CP NMR spectroscopy demonstrated that no additional defects arose within the zeolites after exposure to zinc metal vapour (Figures SI12-14). Overall, the CVD reaction of zinc with ZSM-5, FER and MOR frameworks results in high zinc exchange of the BAS/[NH4]+ cations and does not damage the zeolite framework or block the pore network.

Having demonstrated successful exchange of BAS for Zn^{2+} cations of ZSM-5, FER and MOR, the materials were studied for the capacity to effect C-H activation of methane, following similar conditions to those reported by Stepanov.[10b] After reaction with zinc vapour at 500 °C, the Zn/Zeolite samples were cooled to
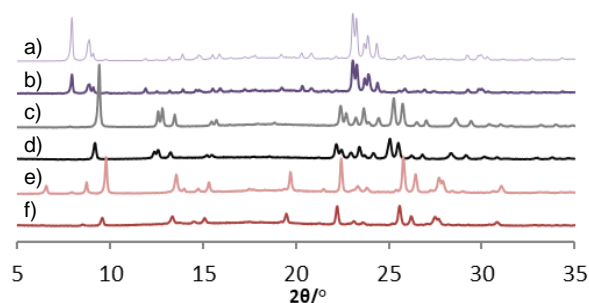

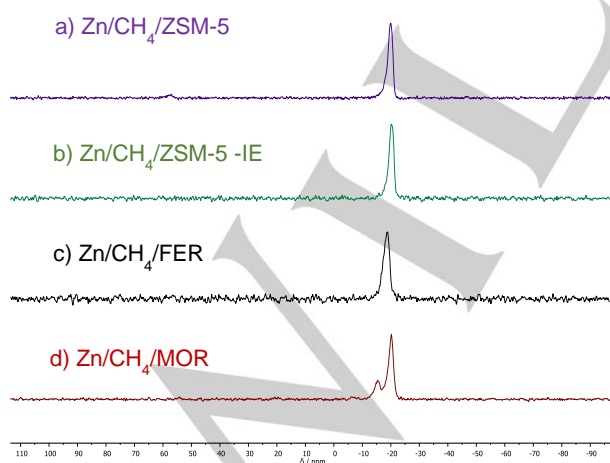Figure 2: pXRD patterns for (a) H-ZSM-5, (b) Zn/ZSM-5, (c) NH4-FER, (d) Zn/FER, (e) H-MOR and (f) Zn/MOR

Figure 3: ^{13}C CP MAS NMR spectra of (a) Zn/CH4/ZSM-5, (b) Zn/CH4/ZSM-5-IE, (c) Zn/CH4/FER and (d) Zn/CH4/MOR. A characteristic signal for the [Zn-CH3]+ species is observed at a chemical shift of around -19 ppm in all spectra.

250 °C and then exposed to $^{13}CH_4$ for 15 minutes. When the Zn/CH4/ZSM-5 CVD sample was analysed by ^{13}C CP MAS NMR spectroscopy we were pleased to observe a signal at −19 ppm (Figure 3a), characteristic of the [Zn-CH3]+ fragment, in line with previous reports.[9-10] Gratifyingly, when the Zn/CH4/FER was likewise analysed, a signal at -20 ppm was also observed (Figure 3c), indicating the successful activation of methane to form the [Zn-CH3]+ fragment. Most excitingly, after exposure to $^{13}CH_4$ analysis of the Zn/CH4/MOR sample showed the presence of two signals at -15 ppm and -20 ppm (Figure 3d). Neither FER or MOR frameworks, modified with zinc, have been previously reported to activate methane. Zn/CH4/ZSM-5-IE, prepared by aqueous ion exchange (IE) of Zn^{2+} ions, also is able to activate methane, as demonstrated by the ^{13}C NMR signal observed at -19 ppm (Figure 3b), in line with observations reported by other groups.[11a, 18] It should be noted that the conditions required to observe C-H activation of methane with the IE sample (Zn/CH4/ZSM-5-IE) were based on those reported in the literature but are substantially different to those required using samples prepared by CVD with zinc vapour. No change is observed in the pXRD patterns after methane activation and for Zn/ZSM-5-IE (SI5-7).

Using hexamethylbenzene (HMB) as a standard, further NMR experiments were carried out to determine the percentage of zinc sites that resulted in the formation of the [Zn-CH3]+ species (Table 1). Details of the quantification calculations can be found in the SI. It was found that 5.7% of the zinc sites in ZSM-5 formed [Zn-CH3]+, in line with values reported in the literature of 5-10%.[18a] The number of active zinc sites in FER and MOR were found to be substantially fewer, 0.8% and 1.2% respectively. This is potentially due to the difference in topology between the three frameworks but other factors such as Al distribution could play a role in this finding.[19] Interestingly, alongside the [Zn-CH3]+ ^{13}C NMR signal observed at -20 ppm in Zn/CH4/MOR, an unexpected second signal was observed at -15 ppm, also in the range expected for a [Zn-CH3]+ species.[20] MOR is a 1D zeolite framework containing 12 MR channels and 8 MR side pockets, both of which are accessible to methane gas (Figure 4a). We hypothesised that the two peaks observed in the ^{13}C NMR spectrum in Zn/CH4/MOR correspond to two [Zn-CH3]+ species contained within these two different framework environments.

Further NMR spectroscopic experiments were carried out to investigate the two signals observed for Zn/CH4 MOR. Through a ^{1}H-^{13}C heteronuclear correlation (HETCOR) MAS NMR experiment (spectrum shown in Figure 4b) it can be seen that there are two discrete [Zn-$^{13}CH_3$]+ environments within Zn/CH4MOR. The ^{1}H signal shows coupling to the ^{13}C nucleus giving a doublet and each environment has a different J-coupling constant: 125 Hz for the main species and 140 Hz for the minor species. Coupling constants are known to be dependent on confinement, therefore, this is likely to correspond to strong confinement of [Zn-CH3]+ species in the 8MR side pockets (140 Hz) compared with [Zn-CH3]+ in the 12 MR main channel (125 Hz).[21]

To confirm the two [Zn-CH3]+ sites could not chemically exchange or transfer magnetisation an EXSY experiment was conducted. The absence of any off-diagonal peaks in Figure 4c indicates no transfer between sites after 200 ms of mixing. This strongly suggests the presence of at least two well separated [Zn-CH3]+ environments within Zn/CH4 MOR.
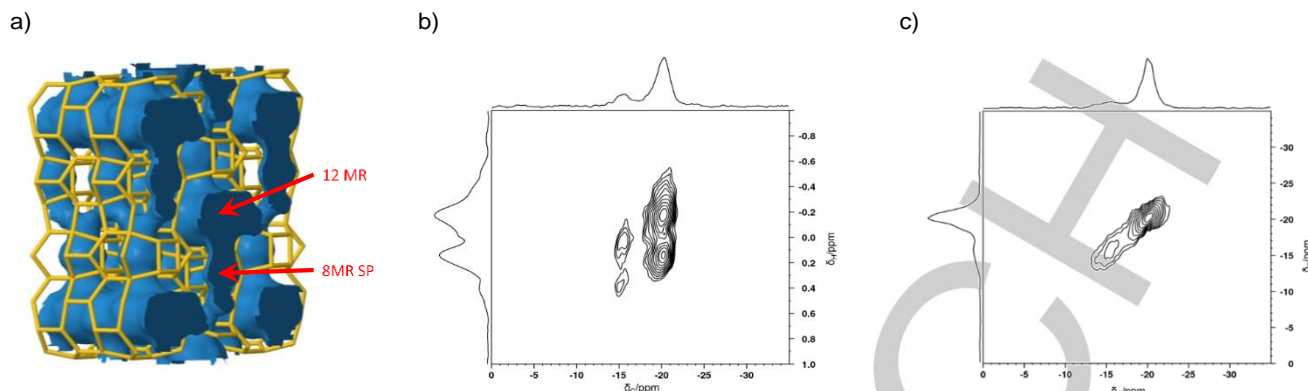
RESEARCH ARTICLE

Figure 4: (a) Framework representation of MOR framework taken from IZA database highlighting the 12MR channel and 8MR SP. (b) ^{1}H-^{13}C heteronuclear correlation (HETCOR) MAS NMR spectrum for Zn/CH$_4$ MOR indicating two distinct [Zn-CH$_3$]$^+$ environments. (c) EXSY experiment of Zn/CH$_4$ MOR highlighting lack of chemical exchange or transfer of magnetisation between the two [Zn-CH$_3$]$^+$ sites.

The distinct topological environments of the 12MR and the 8MR SP within MOR have previously been observed to give rise to two distinct chemical environments, as determined by ^{23}Na and ^{133}Cs MAS NMR spectroscopy studies.[22] Gerstein *et al.* observed two signals in the ^{133}Cs NMR spectrum of fully dehydrated Cs-exchanged mordenite. The peaks are observed in a 1:3 ratio which the authors assigned to the 12MR main channel and 8MR side pocket within the MOR framework.[22b] Two-dimensional triple-quantum (2D-3Q) ^{23}Na MAS NMR spectroscopy of sodium cations in dehydrated Na/MOR also shows two clear signals assigned to Na cations within the 12MR channels and Na cations located in the 8MR side pockets of the mordenite channels.[22a] Overall, based on NMR spectroscopy studies, the two peaks observed for the [Zn-CH$_3$]$^+$ species in MOR correspond to distinct chemical environments likely associated with the 8MR side pocket and 12 MR channels within the zeolite framework.

Reactivity of [Zn-CH$_3$]$^+$ under oxidative conditions

Having determined that zinc modified ZSM-5, FER and MOR are able to activate methane to form well defined [Zn-CH$_3$]$^+$ species, we subsequently explored the reactivity of these species under oxidative conditions. Upon exposure to 20% O$_2$ in Ar at room temperature for 20 minutes, the three zeolites Zn/CH$_4$/O$_2$/ZSM-5, Zn/CH$_4$/O$_2$/FER and Zn/CH$_4$/O$_2$/MOR, showed clear differences in reactivity however the [Zn-CH$_3$]$^+$ signal is still observed in all spectra in Figure 5 after exposure to 20% O$_2$/Ar. Two new signals appear in the ^{13}C CP MAS NMR spectrum of Zn/CH$_4$/O$_2$ ZSM-5 (Figure 5a). These correspond to a zinc methoxy species (54 ppm) and a zinc formate species (173 ppm) which is in line with previous findings on the exposure of [Zn-CH$_3$]$^+$/ZSM-5 to O$_2$.[10b, 12] Conversely, the FER sample shows the presence of a zinc formate peak only (Figure 5b), while the MOR sample exhibits no reactivity towards dioxygen at room temperature after 20 minutes exposure (Figure 6c). This indicates that the framework environment plays a key role in the reactivity of [Zn-CH$_3$]$^+$ with O$_2$ at room temperature, with the MFI framework giving rise to more detectable products than either FER or MOR.

Contrary to this, the Zn/CH$_4$/ZSM-5, Zn/CH$_4$/FER and Zn/CH$_4$/MOR show similar reactivity when the [Zn-CH$_3$]$^+$ species is exposed to O$_2$ (20% in Ar) at 200 °C for 15 min, forming zinc methoxy and zinc formate species with similar spectral intensities

(Figure 6). After a further 12 hours at room temperature the zinc methoxy and zinc formate species in ZSM-5 are still present at comparable intensity indicating further reaction at room temperature is not substantial (Figure 6b) and that the zinc methoxy and zinc formate species are stable at room temperature. The [Zn-CH$_3$]$^+$ species once again does not react fully and can be seen in all spectra. It should also be noted that the two signals discussed previously for the [Zn-CH$_3$]$^+$ species in MOR are both present after each reaction with O$_2$. However, as Figure 7 shows, the species corresponding to the -20 ppm peak appears to be more reactive. The intensity ratio for the -15 ppm and -20 ppm peaks changes from approximately 0.5:1 for the Zn/CH$_4$/MOR to 0.8:1 for the oxygen exposed sample, Zn/CH$_4$/O$_2$/MOR. The spectra in Figure 7 are plotted on equivalent vertical scales after taking into account the differing number of repetitions (800 vs 4000) and the change in relaxation behaviour involved in exposure to oxygen. The differences in loss of signal intensity indicates that they undergo different rates of reaction. As mentioned previously, the signal at –15 ppm is assigned to the [Zn-CH$_3$]$^+$ fragment in the 8MR SP while the signal at –20 ppm is assigned to the [Zn-CH$_3$]$^+$ fragment in the 12MR main channel.
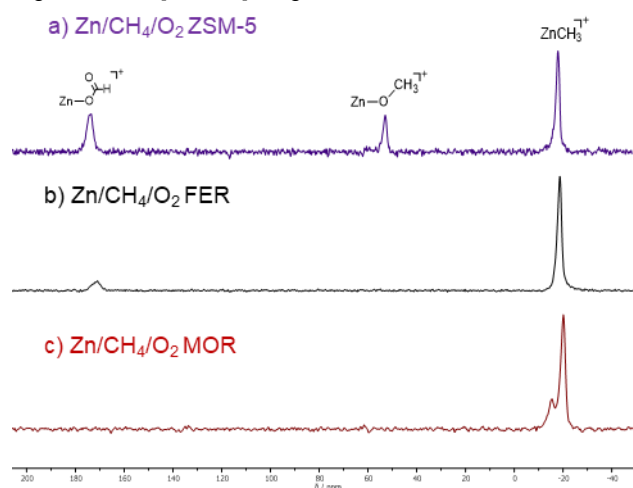

Figure 5: ^{13}C CP MAS NMR spectrum of Zn/CH$_4$/O$_2$ ZSM-5 (a), Zn/CH$_4$/O$_2$ FER (b) and Zn/CH$_4$/O$_2$ MOR (c) after exposure to 20% O$_2$ in Ar at room temperature. Signals corresponding to a methoxy species (54 ppm) and formate species (173 ppm) are observed for ZSM-5 and FER.
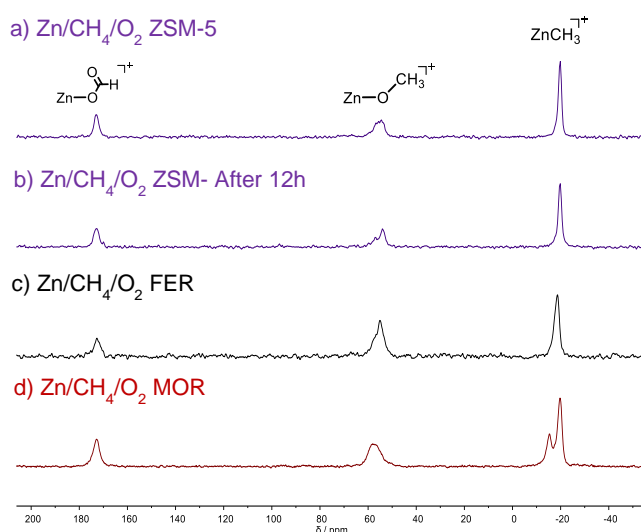
Figure 6: ^{13}C CP MAS NMR spectrum of Zn/CH$_4$/O$_2$ ZSM-5 (a), Zn/CH$_4$/O$_2$ ZSM-5 after 12h (b), Zn/CH$_4$/O$_2$ FER (c) and Zn/CH$_4$/O$_2$ MOR (d) after exposure to 20% O$_2$ in Ar at 200 °C for 15 min. Peaks corresponding to a methoxy species (54 ppm) and formate species (173 ppm) observed in all spectra

Our observations for the [Zn-CH$_3$]$^+$/MOR system indicated confinement stabilises the [Zn-CH$_3$]$^+$ species in the 8MR SP, leading to lower reactivity in the presence of O$_2$.

The reactivity of the [Zn-CH$_3$]$^+$ species was further tested by exposure to air. After zinc vapour deposition and exposure to ^{13}CH$_4$, Zn/CH$_4$/ZSM-5, Zn/CH$_4$/FER and Zn/CH$_4$/MOR were left open to the atmosphere overnight by removal of the NMR rotor cap. The three samples exhibited varying reactivity under these conditions. For both the Zn/CH$_4$/air/ZSM-5 and Zn/CH$_4$/air/FER (Figure 8a and 8b respectively), the signal corresponding to [Zn-CH$_3$]$^+$ is absent and, free MeOH (50 ppm)[12] and zinc formate species have been formed. We note that the Zn/CH$_4$/air/FER spectrum has a higher signal to noise ratio. Zn/CH$_4$/air/MOR proves to be the most interesting sample as it is the only framework which still gives a signal from the [Zn-CH$_3$]$^+$ species after overnight exposure to the atmosphere. Even after 36 h, there is a signal present from residual [Zn-CH$_3$]$^+$ species. The MOR framework is also unique in the fact that predominantly methanol is formed, while trace amounts of zinc formate are observed. The reduced signal intensity of Zn/CH$_4$/air/FER and Zn/CH$_4$/air/MOR after 36 h is likely due to loss of the methanol or protonlysis of the [Zn-CH$_3$]$^+$ species by water to form methane.[12] Furthermore, we
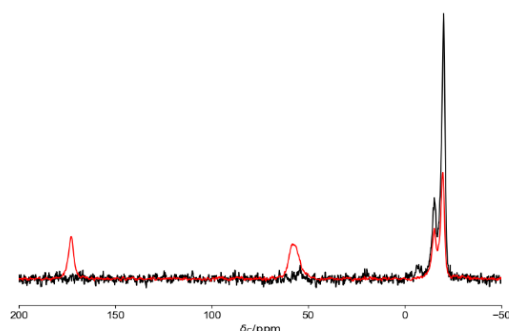
also propose that the complete loss of the signal associated with [Zn-CH$_3$]$^+$ in the air exposure experiments compared to O$_2$/Ar is due to the differences in experimental conditions of O$_2$/Ar exposure (sample sealed under O$_2$/Ar in a capped rotor i.e. limited O$_2$) vs air exposure (sample in an uncapped rotor).

While it is unclear why the differing frameworks display disparate reactivity under different oxidative conditions, these findings highlight that the framework plays a crucial role in the reactivity of the [Zn-CH$_3$]$^+$. The MFI framework seems to be the most reactive environment for the [Zn-CH$_3$]$^+$ species whereas the MOR framework leads to greater methanol selectivity.

Conclusions

Using CVD with an excess of zinc metal, zinc-modified zeolites of three frameworks (ZSM-5, FER and MOR) were prepared with high levels of zinc exchange. After CVD, the materials retained high surface areas, good crystallinity and no additional defects were observed. Upon exposure to ^{13}CH$_4$, C-H activation was observed to occur for all three frameworks, as determined by a characteristic signal resulting from [Zn-CH$_3$]$^+$ in ^{13}C MAS NMR spectroscopy studies. Using HMB as an NMR standard, the percentage of zinc atoms that resulted in the formation of the [Zn-CH$_3$]$^+$ species was determined; the order was found to be Zn/CH$_4$/ZSM-5 (5.7%), Zn/CH$_4$/MOR (1.2%) and Zn/CH$_4$/FER (0.8%). At this stage it is unclear why the ZSM-5 framework results in a substantially greater number of active Zn sites than either MOR or FER but this is potentially due to the difference in topology between the three frameworks or difference in Al distribution for example.

The activation of methane over Zn/MOR proved to be particularly interesting as two signals were observed in the ^{13}C NMR spectrum after exposure to ^{13}CH$_4$. Further NMR spectroscopy experiments determined that these two signals
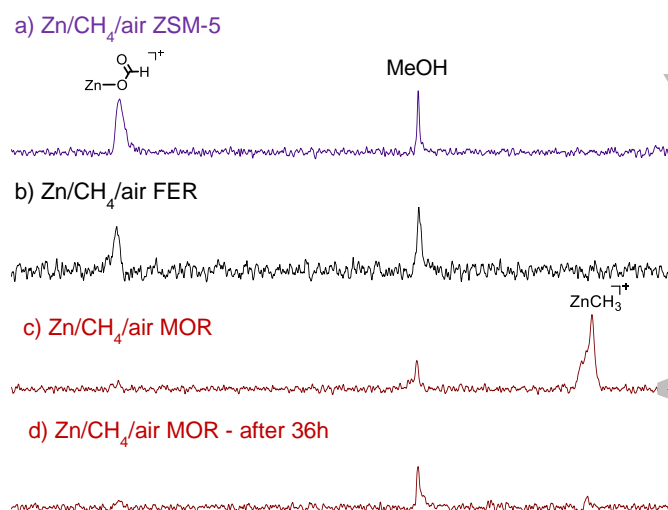

Figure 8: ^{13}C CP MAS NMR spectrum of Zn/CH4/air ZSM-5 (a), Zn/CH4/air FER (b), Zn/CH4/air MOR (c) after exposure to air overnight at room temperature. (d) shows reactivity for Zn/CH4/air MOR after 36h. Signals corresponding to free methanol (50 ppm) and formate species (173 ppm) observed.

Figure 7: ^{13}C CP MAS spectra from Zn/CH$_4$/MOR before (black) and after (red) exposure to 20% O$_2$ in Ar at 200 °C

RESEARCH ARTICLE

belonged to two distinct chemical environments which were unable to chemically exchange and had different J-coupling constants. This fitted with our hypothesis that the two signals are associated with [Zn-CH$_3$]$^+$ species present in the 12 MR channels and the 8MR side pockets of the MOR framework. Additionally, the two species undergo different rates of reaction upon exposure to O$_2$.

After establishing stoichiometric methane activation, the reactivity of the [Zn-CH$_3$]$^+$ species under oxidative conditions was explored. As expected, methoxy and formate species were formed by all three frameworks after exposure to O$_2$ at elevated temperatures. However, the three frameworks demonstrated dissimilar reactivity under different oxidative conditions highlighting that the framework plays a key role in the reactivity of the [Zn-CH$_3$]$^+$ species. ZSM-5 framework was found to be the most reactive environment for the [Zn-CH$_3$]$^+$ species whilst Zn/CH$_4$/air/MOR seemed selective for methoxy species.

Further work will be carried out to investigate the catalytic properties of these materials now stoichiometric methane activation and functionalisation has been proven.

Experimental Section

H–MOR (Si/Al = 10), H–ZSM–5 (15) and NH$_4$–ZSM-5 (12.5) were kindly provided by Clariant. NH$_4$–FER (10) was purchased from Alfa Aesar. Zinc powder (Goodfellow, 99.9%, max particle size 150 μm) was used as purchased. Zinc nitrate hexahydrate (99%) was used as purchased from Alfa Aesar. Methane-^{13}C (99% ^{13}C) was purchased from Sigma-Aldrich. CH$_4$ (99.995%), O$_2$ (99.5%), N$_2$ (oxygen free) and Ar (99.998%) cylinders were purchased from BOC. Zinc powder was stored and used in a PureLab HE glove box under an argon atmosphere.

The ion exchanged ZSM–5 (Zn/ZSM-5-IE) was prepared by treating NH$_4$–ZSM–5 (12.5) with an aqueous solution Zn(NO$_3$)$_2$ based on a method reported by Kuroda et al..[18a] Zinc ion exchanges were carried out using 2.5 g of zeolite in a centrifuge tube in contact with 50 ml of 0.3M Zn(NO$_3$)$_2$ solution for 1 h with constant agitation from a mechanical tube roller. The tube was centrifuged at 4500 rpm for 5.5 min and the resulting supernatant decanted. The zeolite was then re-dispersed into the zinc nitrate solution and this process was repeated 10 times. The sample was then washed with 50 ml of deionised water 8 times and dried at 80 °C overnight. The resulting sample is referred to Zn/ZSM–5 IE. The vapour deposition samples were prepared by an exchange reaction between metallic zinc vapour and the H-form/NH$_4$-form of the zeolite. This was carried out in a custom quartz u-tube which ensured the separation of the zinc powder and zeolite. All parent zeolites were pre-treated in the same way to dehydrate before exposure to zinc vapour. The parent zeolite was placed into a quartz tube under vacuum (pressure < 10^{-2} mbar) and heated to 150 °C for 1 h followed by 5 h at 550 °C in a tube furnace. A 5 °C min^{-1} ramp rate was used for all furnace program steps. After dehydration, the zeolites were stored in the glovebox. The vapour deposition conditions were based on a method reported by Stepanov et al..[10b] To achieve maximum ion exchange, a 100-fold excess of zinc (Zn/Al =100) was used for the vapour deposition. The quartz u-tube and liner used for the reaction are

shown in the supplementary information in Figure SI1. The u-tube was loaded with zinc metal and zeolite in the glovebox, ensuring the powders were well separated on either sides of the tube (see Figure SI1). The u-tube was then attached to a Schlenk line and placed under vacuum (pressure <10^{-2} mbar). To expose the zeolite sample to zinc vapour, the u-tube was sealed and placed in a tube furnace where it was heated to 500 °C at 5 °C min^{-1} and held for 1 h under static vacuum. Excess unreacted zinc vapour was further removed by continued heating at 500 °C for 2 h under dynamic vacuum. These samples are referred to as Zn/ZSM–5, Zn/MOR, Zn/FER.

Where methane activation took place, the u-tube containing the zinc modified zeolite was cooled to 250 °C in the furnace. The u-tube was filled with 1 atm of ^{13}CH$_4$, sealed and held at 250 °C for 15 min. After cooling, the sealed tube was taken into the argon glovebox. These samples, labelled Zn/CH$_4$/ZSM–5, Zn/CH$_4$/MOR, Zn/CH$_4$/FER, were packed into a solid state NMR rotor in the glovebox. NMR experiments were typically conducted immediately after C-H activation.

The ion exchanged sample, Zn/ZSM-5-IE, was activated based on a method by Kuroda et al..[18a] The zeolite was heated to 600 °C for 4 h at 5 °C min^{-1} ramp rate under vacuum. This was cooled to 250 °C after which the tube was sealed under 1 atm of ^{13}CH$_4$ and held at 250C °C for 2 h. After cooling, the sealed tube was taken into the argon glovebox. The sample, labelled Zn/CH$_4$/ZSM–5 IE, was packed into a solid state NMR rotor in the glovebox. NMR experiments were typically conducted immediately after C-H activation.

The [Zn-CH$_3$]$^+$ species in Zn/CH$_4$/ZSM–5, Zn/CH$_4$/MOR and Zn/CH$_4$/FER were tested for reactivity with O$_2$ and air. A solid state NMR rotor containing Zn/CH$_4$/zeolite was placed in a Schlenk flask under a flow of O$_2$/Ar, after removing the rotor cap. This was exposed to a mixture of 20% O$_2$ in Ar flowing at room temperature for 15 min. When testing reactivity at 200 °C, the flask was sealed under the atmosphere of the O$_2$/Ar mixture, and the samples were heated at 200 °C for 15 min. After cooling to room temperature, the rotor was then re-capped under a nitrogen flow. Reactivity with air was tested by removing the rotor cap of samples Zn/CH$_4$/zeolite and leaving the samples exposed to air overnight.

All additional characterisation details are documented in the supplementary information.

RESEARCH ARTICLE

References

[1]   a) G. A. Olah, *Angew. Chem., Int. Ed.* **2005**, *44*, 2636-2639; b) B. A. Arndtsen, R. G. Bergman, T. A. Mobley, T. H. Peterson, *Acc. Chem. Res.* **1995**, *28*, 154-162.

[2]   a) K. Aasberg-Petersen, J. H. Bak Hansen, T. S. Christensen, I. Dybkjaer, P. S. Christensen, C. Stub Nielsen, S. E. L. Winter Madsen, J. R. Rostrup-Nielsen, *Appl. Catal., A* **2001**, *221*, 379-387; b) R. Reimert, F. Marschner, H. J. Renner, W. Boll, E. Supp, M. Brejc, W. Liebner, G. Schaub, in *Gas Production 2. Processes*, *Ullmann's Encyclopedia of Industrial Chemistry*, Wiley-VCH Verlag GmbH & Co. KGaA, **2011**. c) K. Aasberg-Petersen, I. Dybkjær, C. V. Ovesen, N. C. Schjødt, J. Sehested, S. G. Thomsen, *J. Nat. Gas Sci. Eng.* **2011**, *3*, 423-459.

[3]   a) V. C. C. Wang, S. Maji, P. P. Y. Chen, H. K. Lee, S. S. F. Yu, S. I. Chan, *Chem. Rev.* **2017**, 8574–8621; b) M. O. Ross, A. C. Rosenzweig, *J. Biol. Inorg. Chem.* **2017**, *22*, 307-319; c) B. E. R. Snyder, M. L. Bols, R. A. Schoonheydt, B. F. Sels, E. I. Solomon, *Chem. Rev.* **2018**, *118*, 2718-2768.

[4]   a) M. H. Mahyuddin, A. Staykov, Y. Shiota, K. Yoshizawa, *ACS Catal.* **2016**, *6*, 8321-8331; b) P. Tomkins, M. Ranocchiari, J. A. van Bokhoven, *Acc. Chem. Res.* **2017**, *50*, 418-425; c) M. B. Park, S. H. Ahn, A. Mansouri, M. Ranocchiari, J. A. van Bokhoven, *ChemCatChem* **2017**, *9*, 3705-3713; d) S. Raynes, M. A. Shah, R. A. Taylor, *Dalton Trans.* **2019**, *48*, 10364-10384; e) M. Ravi, M. Ranocchiari, J. A. van Bokhoven, *Angew. Chem., Int. Ed.* **2017**, *56*, 16464-16483.

[5]   P. J. Smeets, M. H. Groothaert, R. A. Schoonheydt, *Catal. Today* **2005**, *110*, 303-309.

[6]   a) J. S. Woertink, P. J. Smeets, M. H. Groothaert, M. A. Vance, B. F. Sels, R. A. Schoonheydt, E. I. Solomon, *Proc. Natl. Acad. Sci.* **2009**, *106*, 18908-18913; b) G. Li, P. Vassilev, M. Sanchez-Sanchez, J. A. Lercher, E. J. M. Hensen, E. A. Pidko, *J. Catal.* **2016**, *338*, 305-312.

[7]   a) M. Dusselier, M. E. Davis, *Chem. Rev.* **2018**, 5265–5329; b) M. J. Wulfers, S. Teketel, B. Ipek, R. F. Lobo, *Chem. Commun.* **2015**, *51*, 4447-4450.

[8]   D. K. Pappas, A. Martini, M. Dyballa, K. Kvande, S. Teketel, K. A. Lomachenko, R. Baran, P. Glatzel, B. Arstad, G. Berlier, C. Lamberti, S. Bordiga, U. Olsbye, S. Svelle, P. Beato, E. Borfecchia, *J. Am. Chem. Soc.* **2018**, 15270–15278.

[9]   V. B. Kazansky, A. I. Serykh, *Phys. Chem. Chem. Phys.* **2004**, *6*, 3760-3764.

[10] a) M. V. Luzgin, D. Freude, J. Haase, A. G. Stepanov, *J. Phys. Chem. C* **2015**, *119*, 14255-14261; b) A. A. Gabrienko, S. S. Arzumanov, M. V. Luzgin, A. G. Stepanov, V. N. Parmon, *J. Phys. Chem. C* **2015**, *119*, 24910-24918; c) Y. G. Kolyagin, I. I. Ivanova, Y. A. Pirogov, *Solid State Nucl. Magn. Reson.* **2009**, *35*, 104-112.

[11] a) A. Oda, H. Torigoe, A. Itadani, T. Ohkubo, T. Yumura, H. Kobayashi, Y. Kuroda, *J. Phys. Chem. C* **2013**, *117*, 19525-19534; b) S. C. Albarracín-Suazo, Y. J. Pagán-Torres, M. C. Curet-Arana, *J. Phys. Chem. C* **2019**, *123*, 16164-16171.

[12] J. F. Wu, W. D. Wang, J. Xu, F. Deng, W. Wang, *Chem. - Eur. J.* **2010**, *16*, 14016-14025.

[13] Y. Lin, S. Qi, L. Benedict, Z. Junlin, K. Dejing, M. Claire, T. Chiu, T. Edman, *Angew. Chem., Int. Ed.* **2017**, *56*, 10711-10716.

[14] E. Morra, G. Berlier, E. Borfecchia, S. Bordiga, P. Beato, M. Chiesa, *J. Phys. Chem. C* **2017**, *121*, 14238-14245.

[15] A. Oda, T. Ohkubo, T. Yumura, H. Kobayashi, Y. Kuroda, *Dalton Trans.* **2015**, *44*, 10038-10047.

[16] T. Gullion, *Chem. Phys. Lett.* **1995**, *246*, 325-330.

[17] S. M. T. Almutairi, B. Mezari, P. C. M. M. Magusin, E. A. Pidko, E. J. M. Hensen, *ACS Catal.* **2012**, *2*, 71-83.

[18] a) A. Oda, H. Torigoe, A. Itadani, T. Ohkubo, T. Yumura, H. Kobayashi, Y. Kuroda, *J. Phys. Chem. C* **2014**, *118*, 15234-15241; b) A. A. Gabrienko, S. S. Arzumanov, A. V. Toktarev, I. G. Danilova, I. P. Prosvirin, V. V. Kriventsov, V. I. Zaikovskii, D. Freude, A. G. Stepanov, *ACS Catal.* **2017**, *7*, 1818-1830.

[19] a) E. A. Pidko, R. A. van Santen, *J. Phys. Chem. C* **2007**, *111*, 2643-2655; b) A. Oda, T. Ohkubo, T. Yumura, H. Kobayashi, Y. Kuroda, *Phys. Chem. Chem. Phys.* **2017**, *19*, 25105-25114.

[20] a) Y. G. Kolyagin, I. I. Ivanova, V. V. Ordomsky, A. Gedeon, Y. A. Pirogov, *J. Phys. Chem. C* **2008**, *112*, 20065-20069; b) H. Elmar, *Z. Anorg. Allg. Chem.* **2000**, *626*, 2223-2227.

[21] J. Geertsen, J. Oddershede, W. T. Raynes, G. E. Scuseria, *J. Magn. Reson* **1991**, *93*, 458-471.

[22] a) M. Hunger, P. Sarv, A. Samoson, *Solid State Nucl. Magn. Reson.* **1997**, *9*, 115-120; b) P. J. Chu, B. C. Gerstein, J. Nunan, K. Klier, *J. Phys. Chem.* **1987**, *91*, 3588-3592.

WILEY-VCH

RESEARCH ARTICLE

Entry for the Table of Contents (Please choose one layout)

Layout 2:

RESEARCH ARTICLE
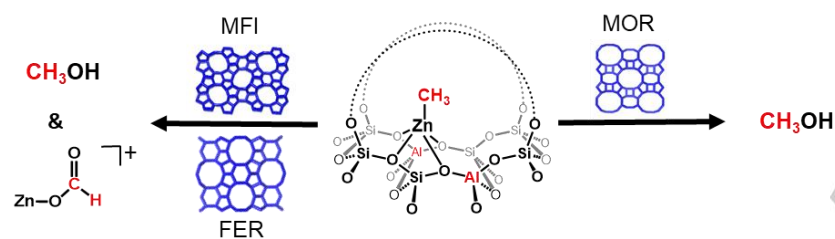
Meera A. Shah, Samuel Raynes, Dr David C. Apperley, Dr Russell A. Taylor*

Page No. – Page No.

Framework Effects on Activation and Functionalisation of Methane in Zinc-Exchanged Zeolites

It's all about the framework! The zeolite framework is shown to influence the number of extraframework zinc species that can activate methane as well as the observed oxidation products. Selective methanol formation is demonstrated utilising the MOR framework.